

Multiphase Characterization of Phosphorus Sulfides by Multidimensional and MAS-³¹P NMR Spectroscopy. Molecular Transformations and Exchange Pathways at High Temperatures[†]

T. Bjorholm*[‡] and H. J. Jakobsen*[§]

Contribution from the Cheminova A/S, P. O. Box 9, DK-7620 Lemvig, Denmark, and Department of Chemistry, University of Aarhus, DK-8000 Aarhus C, Denmark. Received May 29, 1990

Abstract: High-temperature 1D and 2D exchange ³¹P-NMR spectra of pure and well-defined phosphorus sulfides show that, e.g., β-P₄S₅ or mixtures of P₄S₃ and sulfur transform into mixtures of at least eight different P₄S_n (n = 3-7) species which are identified and quantified. Transformations and exchange pathways between the different P₄S_n species in the melts are revealed by the 2D exchange ³¹P-NMR spectra at 225-250 °C. Furthermore, the exchange correlations observed from these spectra yield unambiguous assignments of the unknown or earlier incorrectly assigned ³¹P chemical shifts for β-P₄S₆, β-P₄S₅, α-P₄S₅, and a new P₄S₆ isomer (α-P₄S₆). These assignments are extremely valuable for a correct interpretation of the complex solid-state magic angle spinning (MAS)-NMR spectra of phosphorus sulfides. Two polymorphs for both β-P₄S₅ and β-P₄S₆ (the predominant species in the β-P₄S₅ melt and isolated here for the first time) have been isolated and characterized by high-speed ³¹P MAS-NMR spectroscopy. Molecular distortions, caused by crystal packing and not easily detected by XRD, are observed for all four polymorphs. These distortions cause nonequivalence between phosphorus atoms which are equivalent for the free molecules. Thereby otherwise unobservable isotropic ¹J(P,P)'s have been determined from solid-state NMR spectroscopy.

Phosphorus and sulfur form a fascinating series of P₄S_n (3 ≤ n ≤ 10) compounds which have been studied extensively by different spectroscopic techniques over the years. Some of these phosphorus sulfides are produced in thousands of tons per year from high-temperature melts of the elements and used in manufacturing of insecticides, lubricating oil, additives, plasticizers, flame retardants, etc. Depending on the employed molar ratios of phosphorus and sulfur, very complex mixtures of phosphorus sulfides are obtained. Because these mixtures are difficult to analyze, especially in the molten state, the exact P₄S_n compositions for the melts are only partly understood.

Solution-state ³¹P NMR spectra have been reported for P₄S₃,¹ α-P₄S₄,² β-P₄S₄,² α-P₄S₅,³ β-P₄S₅,⁴ P₄S₇,^{3,5} P₄S₈⁶ (unstable), P₄S₉,⁷ and P₄S₁₀⁷ (molecular structures shown in Figure 1). The spectral assignment of the ³¹P resonances for P₄S₃, α-P₄S₄, β-P₄S₄, P₄S₉, and P₄S₁₀ is straightforward and unambiguous from the molecular symmetries, relative intensities, and one-bond ³¹P-³¹P scalar couplings. From the data of these compounds it is obvious that no simple relationship exists between the ³¹P chemical shifts and the various phosphorus moieties in the different P₄S_n species. Consequently, the assignments of ³¹P NMR spectra of already well-known (e.g., α-P₄S₅,³ β-P₄S₅,⁴ and P₄S₇) and potentially new P₄S_n species are often restricted to indirect evidences and assumptions based on comparison with the data for the unambiguously assigned species.

Infrared and Raman investigations⁸⁻¹¹ have shown that the phosphorus sulfides transform during melting into a series of P₄S_n species. Although the compositions of these melts are usually very complex and only the predominant compounds have been identified by these techniques, the existence of β-P₄S₆ in some of the melts is indisputable. However, β-P₄S₆ has not been isolated until now, and no ³¹P NMR data have been reported so far for this species.

Complementary to the early solution-state ³¹P NMR studies there has recently been a renewed interest in a series of P₄S_n compounds from a solid-state ³¹P magic angle spinning (MAS) point of view. Detailed reports have been given for the ³¹P MAS-NMR spectra for P₄S₃,¹²⁻¹⁴ α-P₄S₅,¹³ P₄S₇,^{5,12,13} P₄S₉,¹² and P₄S₁₀.¹² Because of the high spectral complexity attributable to crystallographically nonequivalent phosphorus atoms, crystal-packing distortions, and large ³¹P chemical shift anisotropies

(CSA's), these spectra can yield valuable information pertinent to the solid state of the compounds. However, an unambiguous assignment of the many resonances in these highly complex spectra is a prerequisite for a correct interpretation of the data.

In the present work we have studied the 1D and 2D exchange (NOESY) ³¹P NMR spectra of high-temperature melts for β-P₄S₅ and for two mixtures of P₄S₃ and sulfur. The result of these investigations in a clear-cut way identifies the transformation products and establishes exchange pathways between the different P₄S_n species generated in the melts. Furthermore, the correlation of the ³¹P chemical shifts for the P₄S_n species obtained from the exchange-correlated spectra permits unambiguous assignments of the ³¹P NMR spectra for β-P₄S₆, β-P₄S₅, and α-P₄S₅ and the identification of a hitherto unknown P₄S₆ isomer (α-P₄S₆, Figure 1). We also report the ³¹P MAS-NMR spectra of two polymorphic forms of β-P₄S₆, isolated for the first time as a solid during this investigation, and of two polymorphic forms of β-P₄S₅, one well-known⁴ and the other isolated during the course of this study.

- (1) Heckmann, G.; Fluck, E. Z. *Naturforsch.* **1971**, *26B*, 982-986.
- (2) Griffin, A. M.; Minshall, P. C.; Sheldrick, G. M. *J. Chem. Soc., Chem. Commun.* **1976**, 809-810.
- (3) Thamm, R.; Heckmann, G.; Fluck, E. *Phosphorus Sulfur* **1981**, *11*, 273-278.
- (4) Griffin, A. M.; Sheldrick, G. M. *Acta Crystallogr. Sect. B* **1975**, *31*, 2738-2740.
- (5) Bjorholm, T. *Chem. Phys. Lett.* **1988**, *143*, 259-262.
- (6) Barieux, J.-J.; Démarcq, M. C. *J. Chem. Soc., Chem. Commun.* **1982**, 176-177.
- (7) Andrew, E. R.; Vennart, W.; Bonnard, G.; Croiset, R. M.; Demarcq, M. C.; Mathieu, E. *Chem. Phys. Lett.* **1976**, *43*, 317-320.
- (8) Gardner, M. *J. Chem. Soc., Dalton Trans.* **1973**, 691-696.
- (9) Bues, W.; Somer, M.; Brockner, W. *Z. Anorg. Allg. Chem.* **1981**, *476*, 153-158.
- (10) Bues, W.; Somer, M.; Brockner, W. *Z. Naturforsch.* **1981**, *36a*, 842-845.
- (11) Somer, M.; Bues, W.; Brockner, W. *Z. Naturforsch.* **1983**, *38a*, 163-166.
- (12) Eckert, H.; Liang, C. S.; Stucky, G. D. *J. Phys. Chem.* **1989**, *93*, 452-457.
- (13) Harris, R. K.; Wilkes, P. J.; Wood, P. T.; Woollins, J. D. *J. Chem. Soc., Dalton Trans.* **1989**, 809-813.
- (14) Bjorholm, T.; Jakobsen, H. J. *J. Magn. Reson.* **1989**, *84*, 204-211.
- (15) Jakobsen, H. J.; Langer, V.; Daugaard, P. *J. Magn. Reson.* **1988**, *76*, 162-168; U.S. Patent Number 4,739,270, April 19, 1988.
- (16) Hazell, R. G. Department of Chemistry, University of Aarhus, DK-8000 Aarhus C, Denmark, to be published.

[†] Presented at the "31st ENC", Asilomar, CA, April 1990.

[‡] Cheminova A/S.

[§] University of Aarhus.

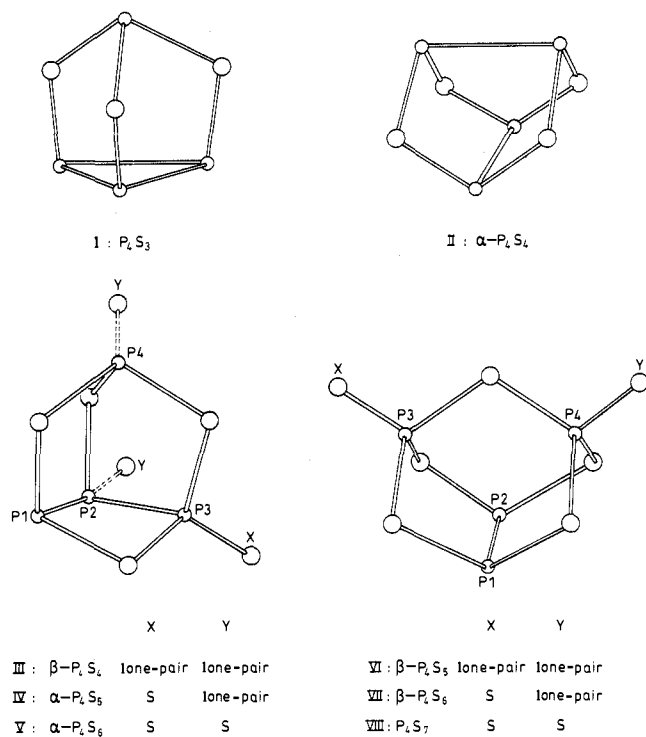


Figure 1. Molecular structures of the phosphorus sulfides discussed and studied in this work. The numbering of the P atoms and of the P_4S_n species corresponds to that used throughout the text, figures, and tables.

Experimental Section

Preparation of the Phosphorus Sulfides. P_4S_3 was purchased from Fluka and purified by recrystallization from CS_2 . $\alpha-P_4S_5$ and P_4S_7 were prepared following the procedures outlined in the literature.³ $\beta-P_4S_5$ was obtained by desulfurization of P_4S_7 .⁹ The hitherto nonisolated $\beta-P_4S_6$ was prepared from P_4S_7 according to the following procedure. A suspension of P_4S_7 in CS_2 was reacted under reflux with an equimolar quantity of $(C_6H_5)_3P$, added dropwise as a solution in CS_2 during 30 min. After evaporation of the solvent, the material was recrystallized from CS_2 to yield yellow crystals of $\beta-P_4S_6$. The crystals showed no well-defined melting point because of the molecular transformations and exchange processes observed at high temperatures (vide supra). The purity of $\beta-P_4S_6$ as well as for $\beta-P_4S_5$ was assessed by solution-state (CS_2) ^{31}P NMR spectroscopy. Several batches of both $\beta-P_4S_5$ and $\beta-P_4S_6$ were prepared. Whereas no impurities could be detected for the samples of $\beta-P_4S_5$, the optimum purity of $\beta-P_4S_6$ was approximately 90–92%, with $\beta-P_4S_5$ and P_4S_7 constituting unavoidable impurities by the method of preparation.

Solution and High-Temperature ^{31}P -NMR Spectroscopy. Room-temperature solution-state and high-temperature molten-state ^{31}P NMR spectra were acquired on a Bruker AC 250 spectrometer by using a specially designed high-temperature (maximum 400 °C) water-cooled 5-mm probe selectively tuned to the ^{31}P frequency of 101.3 MHz. The temperature stability was better than ± 2 °C. The duration of the $\pi/2$ pulse was 5 μs . The molten-state spectra were recorded in an unlocked mode, and for the 1D spectra a 2- μs pulse and a relaxation delay of 100 s were used to ensure full recovery of the magnetization. A temperature of ca. 200 °C was employed for the 1D spectra since this gives optimum resolution (minimum line widths) for the spectra. The 2D ^{31}P exchange spectra were acquired by using the pulse sequence NOESYPH from the Bruker software. The relaxation delay was 2–4 s. To suppress correlation effects from scalar couplings the mixing time τ_m (generally about 100–200 ms) was randomly varied by 10–20%. The temperature for the 2D experiments was increased to ca. 250 °C in order to obtain appropriate exchange rates for the molecular transformations during τ_m . To avoid air contact in the molten state, the solid samples were degassed and sealed under vacuum in heavy-wall NMR tubes. ^{31}P chemical shifts for the CS_2 solutions are referenced to an external sample of 85% H_3PO_4 . Chemical shifts for the melts are referenced via the high-frequency singlet observed for P_4S_7 and taken as 111.1 ppm relative to 85% H_3PO_4 .

Solid-State ^{31}P MAS-NMR Spectroscopy. ^{31}P MAS-NMR spectra were obtained on a Varian XL-300 spectrometer (7.1 T) at 121.42 MHz by using a home-built high-speed spinning CP/MAS probe.¹⁵ Cylindrical 7 mm o.d. Si_3N_4 rotors with a sample volume of 220 μL and spinning

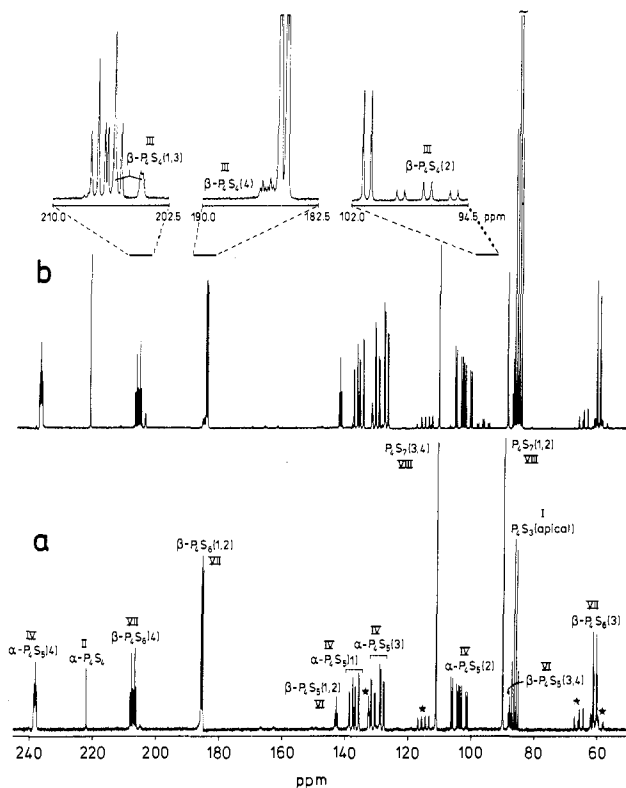


Figure 2. The 101.3 MHz ^{31}P NMR spectra of melts of (a) $\beta-P_4S_5$ and (b) of a 1:1 molar mixture of P_4S_3 and sulfur ($P_4S_{4.0}$) recorded at 196 °C after the samples have been held at 250 °C for 30 min in the probe. The high-frequency singlet for P_4S_7 (111.1 ppm) has been used as reference. The numbers in parentheses indicate the individual ^{31}P resonances of the P_4S_n species and correspond to the labeling of the phosphorus nuclei shown in Figure 1. The four multiplets indicated by asterisks (*) in spectrum (a) correspond to the ABMX spin system of the novel P_4S_6 isomer, $\alpha-P_4S_6$ (see text). To visualize all minor P_4S_n constituents in spectrum (b), the full intensity of the inner lines of the 1:3:3:1 quartet for P_4S_3 (apical) is not shown. Vertical and 7.5-ppm horizontal expansions of the three multiplets for $\beta-P_4S_4$ are shown as insets in spectrum (b).

speeds in the range from 4.0 to 9.5 kHz were employed. A pulse width of 3 μs , corresponding to a 35° flip angle, and a relaxation delay of 20 s were used for all samples. The ^{31}P chemical shift scale was referenced to an external sample of 85% H_3PO_4 by substitution.

Results and Discussion

High-Temperature Melts. Figure 2a shows the 1D ^{31}P NMR spectrum of $\beta-P_4S_5$ recorded at 196 °C after the sample has been heated to 250 °C in the probe for about 30 min. This spectrum clearly indicates that the $\beta-P_4S_5$ melt disproportionates in a clean way to a series of P_4S_n species. The corresponding spectra for the two mixtures of P_4S_3 and sulfur with overall compositions $P_4S_{3.6}$ and $P_4S_{4.0}$, respectively, show a similar appearance albeit the mutual ratios of the P_4S_n compounds are different. The spectrum of the mixture with the overall composition of $P_4S_{4.0}$ is shown in Figure 2b. An unambiguous assignment of the ^{31}P 1D spectra, and thereby of the P_4S_n species in the melts, follows in a straightforward manner from comparison of the ^{31}P resonances (multiplets) in Figure 2 with the solution-state data in the literature^{1–5} and, furthermore, from the 2D exchange spectra (vide infra). The only exceptions for a direct comparison with the literature data are the predominant species in the $\beta-P_4S_5$ melt, shown to be $\beta-P_4S_6$, and a new P_4S_6 isomer (vide infra). The assignment of the ^{31}P resonances to the different P_4S_n species in the melts are indicated in Figure 2a, whereas their molar ratios (%), obtained by integration, are listed in Table I. These percentages account exactly for the sulfur content of the melts. ^{31}P chemical shifts and ^{31}P – ^{31}P coupling constants for the P_4S_n species observed in the melts (196 °C) are summarized in Table II; for comparison their CS_2 solution-state data are also given.

Table I. Compositions of P_4S_n Species (mol %) in Melts of β - P_4S_5 and P_4S_3 + Sulfur^a at 196 °C

		β - P_4S_5	$P_4S_{4,0}$	$P_4S_{3,6}$
I:	P_4S_3	23	55	68
II:	α - P_4S_4	1	1	1
III:	β - P_4S_4		2	2
IV:	α - P_4S_5	25	19	14
V:	α - P_4S_6	16	5	2
VI:	β - P_4S_5	3	3	2
VII:	β - P_4S_6	26	12	8
VIII:	P_4S_7	6	3	2

^a Compositions: 1.14 g of P_4S_3 + 0.16 g of sulfur ($P_4S_{4,0}$), and 1.00 g of P_4S_3 + 0.09 g of sulfur ($P_4S_{3,6}$).

The ^{31}P solution-state (CS_2) spectrum of the β - P_4S_6 crystals obtained by partial desulfurization of P_4S_7 (see Experimental Section) gives an AM_2X spin system which exactly matches the spectrum observed for the predominant species in the β - P_4S_5 melt. There is no direct experimental evidence (e.g., from 2D exchange spectra) for the assignment of P3 and P4 for β - P_4S_6 . However, comparison of the two-bond ^{31}P - ^{31}P coupling constants determined for β - P_4S_5 (45.0 Hz) and P_4S_7 (0.9 Hz) with the related couplings for β - P_4S_6 (46.3 and 11.1 Hz) leads to the assignment of the P3 and P4 resonances for β - P_4S_6 given in Table II. The existence of β - P_4S_6 in the molten state of β - P_4S_5 and of different P_4S_4 isomers has earlier been established by Bues et al.^{9,10} by using infrared and Raman spectroscopy. They showed that β - P_4S_5 and the P_4S_4 isomers decompose during melting into complex mixtures of phosphorus sulfides of which P_4S_3 , P_4S_7 , and β - P_4S_6 were identified.

The similarity between the NMR spectra of the three melts studied here indicates that the transformation products may exist as reversible equilibria. The 2D ^{31}P NMR exchange spectrum of the melt of β - P_4S_5 at 250 °C (Figure 3) confirms this suggestion in that exchange networks for several of the P_4S_n species can be mapped out. It is evident from this spectrum that the disproportionation of β - P_4S_5 involves the insertion of one and two exocyclic sulfur atoms with the formation of β - P_4S_6 and P_4S_7 , respectively, as revealed by cross-peaks for the following equilibrium in Scheme I.

In a recent solid-state ^{31}P MAS investigation on P_4S_7 ⁵ we have unambiguously (re)assigned the CS_2 solution-state ^{31}P resonances for P_4S_7 at 84.7 and 111.1 ppm to P1,P2 and P3,P4, respectively. By using these diagonal peaks (singlets at 89.6 and 111.1 ppm in the melt at 196 °C) as starting points, the assignment of the ^{31}P resonances in β - P_4S_6 and β - P_4S_5 given in Table II are obtained. The intense cross-peak observed between P3 and P4 in β - P_4S_6 reflects exchange of the position for the terminal sulfur atom in this molecule (most likely intramolecular). By this interchange the chemical shift for P1 and P2 is unaffected as the symmetry of the molecule is preserved.

Table II. ^{31}P Chemical Shifts and ^{31}P - ^{31}P Coupling Constants^a for β - P_4S_4 , α - P_4S_5 , α - P_4S_6 , β - P_4S_5 , β - P_4S_6 , and P_4S_7 in Solution^b and in Melts (196 °C)^c

	β - P_4S_4		α - P_4S_5		α - P_4S_6		β - P_4S_5		β - P_4S_6		P_4S_7	
	solution ^d	melt	solution	melt	solution ^d	melt	solution	melt	solution	melt	solution	melt
δ (P1)	207.5	205.0	124.9	136.9	54.9	65.7	129.8	142.3	178.2	184.8	84.7	89.2
δ (P2)	85.7	97.0	91.7	103.6	57.9	59.3	129.8	142.3	178.2	184.8	84.7	89.2
δ (P3)	207.5	205.0	127.0	129.8	115.8	114.9	80.1	87.2	55.7	61.0	111.1	111.1
δ (P4)	174.7	185.8	233.8	237.4	133.5	132.3	80.1	87.2	198.9	206.7	111.1	111.1
J (P1,P2)	168.7	173.8	-184.7 ^e	(-189.3)	152.9	158.2						
J (P1,P3)			119.0	113.0	124.9	125.0	45.0	42.3	11.1	14.1	0.9	5.9
J (P1,P4)	18.1	16.5	19.0	19.5	2.2	7.2	45.0	42.3	46.3	45.1	0.9	5.9
J (P2,P3)	168.7	173.8	-285.4 ^e	(-289.6)	239.8	245.0	45.0	42.3	11.1	14.1	0.9	5.9
J (P2,P4)	50.5	51.3	53.3	52.3	20.0	25.8	45.0	42.3	46.3	45.1	0.9	5.9
J (P3,P4)	18.1	16.5	27.9	30.4	19.1	17.1			113.3	108.9		
rms error	0.25	0.84	0.03	0.41	0.05	0.57	0.20	0.34	0.31	0.31	0.05	0.40

^a All spectral parameters result from iterative computer fitting of the ^{31}P line frequencies for the relevant four-spin systems corresponding to the structures shown in Figure 1; chemical shifts are in ppm and coupling constants in Hz; rms errors are given in the last row of the table. ^b Saturated solutions using CS_2 as solvent with chemical shifts relative to 85% H_3PO_4 . ^c Chemical shifts for the melt are referenced via the high-frequency singlet (taken as 111.1 ppm relative to 85% H_3PO_4) for P_4S_7 observed in the spectrum. ^d From dissolution of the cooled melt in CS_2 . ^e The negative sign for J (P1,P2) and J (P2,P3) follows from the analysis of the ABMX spin system observed at low field (2.3 T; ^{31}P at 40 MHz).³ Note that the spectrum has been reassigned compared to the results in ref 3 (see text).

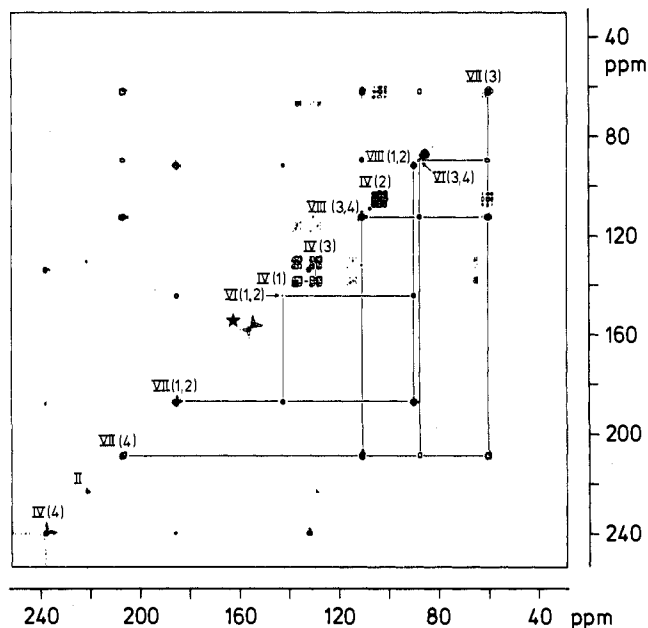
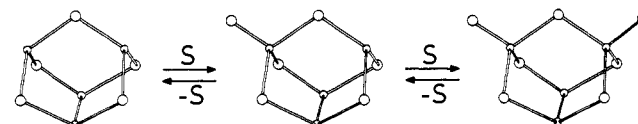


Figure 3. Phase-sensitive 2D exchange ^{31}P NMR spectrum of a melt of β - P_4S_5 at 250 °C (after equilibration for about 30 min at this temperature) obtained by using a mixing time $\tau_m = 100$ ms. The assignments, given along the diagonal, correspond to the formulas shown in Figure 1 with the individual ^{31}P nuclei indicated in parentheses. For comparison see the 1D ^{31}P spectrum in Figure 2a. The signal indicated by an asterisk (*) is the fold-in for the basal doublet of P_4S_3 . The connecting lines for the exchange equilibria β - $P_4S_5 \rightleftharpoons \beta$ - $P_4S_6 \rightleftharpoons P_4S_7$ are drawn as examples.

Scheme I

The 2D ^{31}P NMR exchange spectrum of the melt with composition $P_4S_{4,0}$ (recorded at 225 °C and $\tau_m = 0.2$ s, Figure 4) displays the same exchange networks as observed for the β - P_4S_5 melt. However, for this melt the concentration of β - P_4S_4 has increased to a level that allows transformation cross-peaks to be observed between P1,P3 in β - P_4S_4 and the two separate P1 and P3 resonances for α - P_4S_5 . Unfortunately, the resonances for P1,P3 in β - P_4S_4 and P4 in β - P_4S_6 partly overlap as seen in the Figure 4 2D exchange spectrum; however, on the expanded contour plot and a plot of the slice (at 205.3 ppm) through the diagonal peak for P1,P3 in β - P_4S_4 , shown in Figure 5, the correlation is easily recognized. In addition, further evidence for the transformation

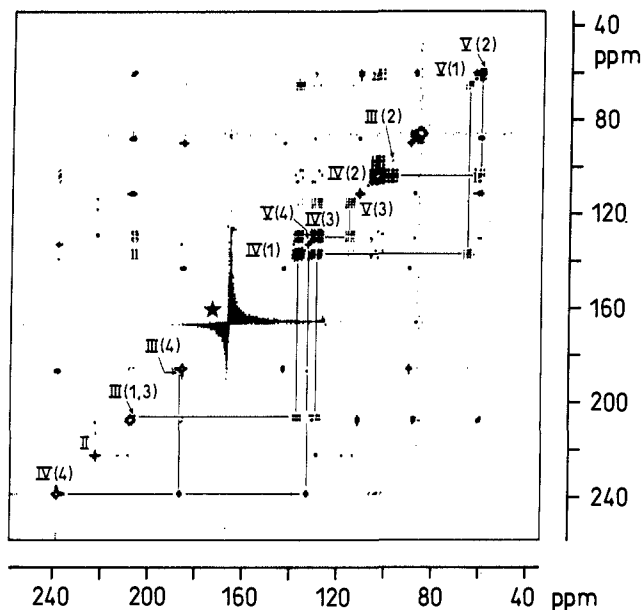


Figure 4. Phase-sensitive 2D exchange ^{31}P NMR spectrum of a melt of the 1:1 molar mixture of P_4S_3 and sulfur ($\text{P}_4\text{S}_{4.0}$) at 225 °C (after equilibration for about 30 min at 250 °C) obtained by using a mixing time $\tau_m = 200$ ms. The assignments, given along the diagonal, correspond to the formulas shown in Figure 1 with the individual ^{31}P nuclei indicated in parentheses. Some assignments and chemical exchange equilibria already shown in Figure 3 are not indicated here. The signal indicated by an asterisk (*) is the fold-in for the basal doublet of P_4S_3 . The connecting lines for the exchange processes $\beta\text{-P}_4\text{S}_4 \rightleftharpoons \alpha\text{-P}_4\text{S}_5 \rightleftharpoons \alpha\text{-P}_4\text{S}_6$ are drawn as examples.

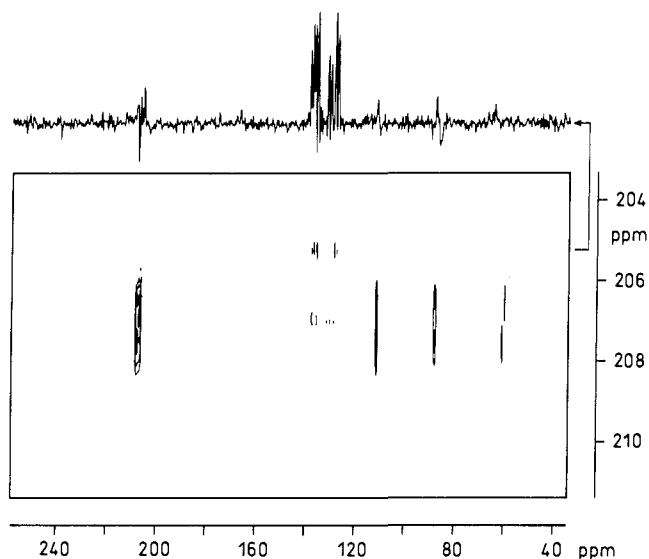
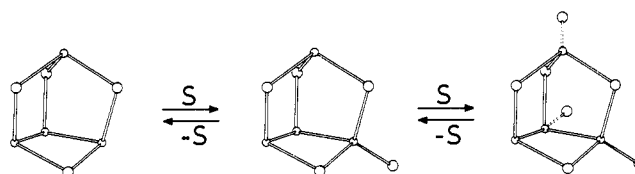


Figure 5. Expansion of the contour plot for the 2D exchange ^{31}P NMR spectrum in Figure 4. A plot of the slice through the diagonal for P1, P3 in $\beta\text{-P}_4\text{S}_4(\text{III})$ at 205.3 ppm is shown above the expanded contour plot (see text).

$\beta\text{-P}_4\text{S}_4 \rightleftharpoons \alpha\text{-P}_4\text{S}_5$ is obtained (Figure 4) from observations of cross-peaks between the P4 (and P2) resonances in $\beta\text{-P}_4\text{S}_4$ and $\alpha\text{-P}_4\text{S}_5$. Although the assignment of the A_2MX spin system for $\beta\text{-P}_4\text{S}_4$ is unambiguous (based on the J_{pp} 's; see also Figure 2b), the 2D exchange spectrum produces no information about the mutual assignment of the resonances for P1 and P3 in $\alpha\text{-P}_4\text{S}_5$. However, assignment of the multiplet at 129.8 ppm to P3 and the multiplet at 136.9 ppm to P1 for $\alpha\text{-P}_4\text{S}_5$ brings the spin-spin couplings $^2J(\text{P1}, \text{P4})$ and $^2J(\text{P2}, \text{P4})$ close to the corresponding values observed in $\beta\text{-P}_4\text{S}_4$.²

Analogously to the (intramolecular) interconversion observed for $\beta\text{-P}_4\text{S}_6$ a similar rearrangement is seen for $\alpha\text{-P}_4\text{S}_5$ by virtue of the cross-peak between the resonances at 129.8 (P3) and 136.9

Scheme II



ppm (P1). The presence of less than 1% $\beta\text{-P}_4\text{S}_4$ in the $\beta\text{-P}_4\text{S}_5$ melt strongly indicates that the symmetric exchange process for $\alpha\text{-P}_4\text{S}_5$ is dominated by an intramolecular mechanism.

For all 2D exchange spectra cross-peak intensities are observed between resonances for $\alpha\text{-P}_4\text{S}_5$ and those of an unknown ABMX spin system. Owing to the lack of symmetry and bearing in mind that all exchange processes observed in the 2D exchange spectra involve formation/breaking (rearrangement) of double bonds between sulfur and phosphorus ($\text{P}=\text{S}$), this species is most probably a novel P_4S_6 isomer ($\alpha\text{-P}_4\text{S}_6$) derived from $\alpha\text{-P}_4\text{S}_5$ by insertion of an exocyclic sulfur at P2 or P4.

In addition to the equilibrium depicted in Scheme I the 2D exchange spectrum of the $\text{P}_4\text{S}_{4.0}$ melt reveals an additional equilibrium based on the $\beta\text{-P}_4\text{S}_4$ cage (Scheme II).

The only known phosphorus sulfide with the $\alpha\text{-P}_4\text{S}_4$ cage is $\alpha\text{-P}_4\text{S}_4$ itself. However, weak cross-peak intensities are observed in Figure 4 between $\alpha\text{-P}_4\text{S}_4$ and an unknown P_4S_n species. The very low concentration of this new compound in the melts (<0.3 mol %) makes evaluation of the spectral parameters difficult. However, expansions (not shown) of the low-intensity resonances in the Figure 2b 1D spectrum at $\delta = 210.0$ ppm (doublet, $^1J(\text{P}, \text{P}=\text{S}) = 452$ Hz, of triplets, $^2J(\text{P}, \text{P}) = 28$ Hz) and $\delta = 115.9$ ppm (doublet, $^1J(\text{P}, \text{P}=\text{S}) = 452$ Hz, of triplets, $^2J(\text{P}, \text{P}) = 12.9$ Hz) clearly indicate that the spin system is obviously of the type AM_2X (it is noted that the corresponding doublet of doublets (M_2 part) at $\delta = 128.5$ ppm could not be observed in the 1D ^{31}P spectrum because of serious overlap in this crowded region of the spectrum). We therefore assume that this species is a P_4S_5 isomer based on the $\alpha\text{-P}_4\text{S}_4$ cage with a doubly bonded sulfur atom at one of the equivalent phosphorus nuclei in $\alpha\text{-P}_4\text{S}_4$. An interesting feature of this AM_2X spin system is the large one-bond coupling $^1J(\text{P}, \text{P}=\text{S}) = 452$ Hz.

The spectral parameters for all P_4S_n species listed in Table II indicate that while the ^{31}P chemical shifts in phosphorus sulfides show large incongruities between similar types of phosphorus atoms in related environments, there is a reasonable agreement between the corresponding ^{31}P - ^{31}P scalar couplings. We note that the assignment of the $\alpha\text{-P}_4\text{S}_5$ spectrum resulting from the present investigations (Table II) disagrees with that proposed earlier by Thamm et al.³ Their assignment is based on the view that $\text{S}=\text{PS}_2$ units normally have chemical shifts below 100 ppm. This obviously is inconsistent with the 2D exchange spectrum. Thamm et al.³ used the same argument in their assignment of the P_4S_7 solution-state (CS_2) spectrum. In a recent study,⁵ however, we unambiguously reassigned the resonances for P_4S_7 and showed that the $\text{S}=\text{PS}_2$ unit for this species has a chemical shift of 111.1 ppm (CS_2 solution).

Finally, we note that distinct changes between the chemical shifts for the molten and liquid states are observed for most of the P_4S_n species.

Solid-State ^{31}P MAS-NMR. High-resolution solid-state ^{31}P MAS-NMR spectra for some of the P_4S_n species generated from the molten-state transformations (vide supra) have recently been reported (P_4S_3 ,¹²⁻¹⁴ $\alpha\text{-P}_4\text{S}_5$,¹³ and P_4S_7 ,^{5,12,13}). In general the complexity of P_4S_n MAS spectra is much higher than their solution-molten-state counterparts. However, new and valuable information, such as ^{31}P - ^{31}P scalar couplings between symmetry-related P atoms for the free molecules (e.g., for P_4S_7), may be extracted from the solids provided a valid interpretation of the spectra is possible. In this respect the results of our molten-state 1D and 2D exchange studies are helpful. Here we report ^{31}P MAS results for the solid phases of some of the important species generated in the melts, i.e., the isomeric and polymorphic forms

Table III. Isotropic ^{31}P Chemical Shifts^a and One-Bond ^{31}P - ^{31}P Scalar Coupling Constants^b from ^{31}P MAS-NMR of α - P_4S_5 and Polymorphs of β - P_4S_5 and β - P_4S_6

	α - P_4S_5^c	β - $\text{P}_4\text{S}_6(\text{A})$	β - $\text{P}_4\text{S}_5(\text{B})$	β - $\text{P}_4\text{S}_6(\text{A})$	β - $\text{P}_4\text{S}_6(\text{B})$
$\delta(\text{P1})$	141.5 (139.8)	146.4	152.3	191.9	192.0
$\delta(\text{P2})$	112.3 (111.4)	146.4	139.8	183.9	178.6
$\delta(\text{P3})$	118.9 (120.2)	98.7	96.5	65.2	70.4
$\delta(\text{P4})$	234.2 (232.7)	75.4	82.5	210.6	193.7
$^1J(\text{P1},\text{P2})^d$	235 (195)		230	320	225

^a Chemical shifts are in ppm (± 0.1 ppm) and referenced to an external sample of 85% H_3PO_4 by substitution. ^b Coupling constants are in Hertz with errors of ca. ± 10 Hz. ^c ^{31}P MAS-NMR parameters for the α - P_4S_5 isomer are reported for comparison with recent literature¹³ values; the latter are shown in parentheses. ^d For α - P_4S_5 the one-bond coupling constant $^1J(\text{P2},\text{P3}) = 275$ Hz (250 Hz¹³).

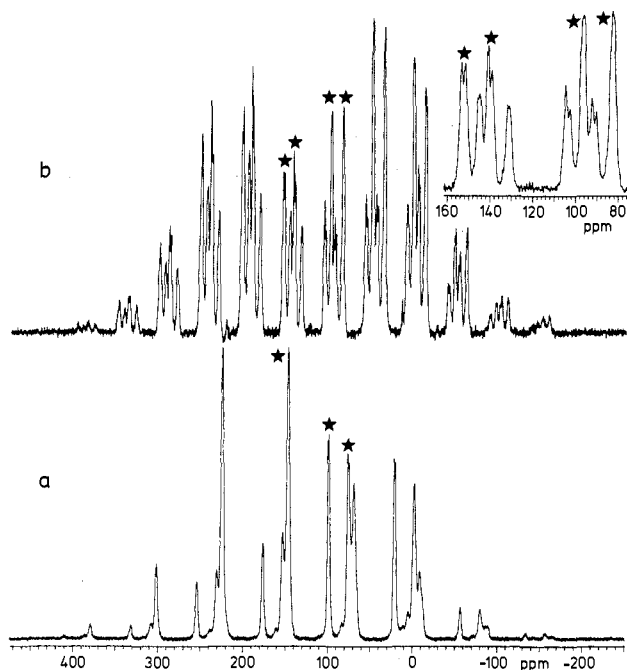


Figure 6. The 121.42 MHz ^{31}P MAS-NMR spectra of two polymorphs of solid β - P_4S_5 : (a) β - $\text{P}_4\text{S}_5(\text{A})$ (200 mg), spinning speed 9425 Hz, 256 transients and (b) β - $\text{P}_4\text{S}_5(\text{B})$ (80 mg), spinning speed 5900 Hz, 2900 transients. An expansion of the region for the four centerbands is shown as an inset. For both spectra 45° pulses of 3- μs pulse width, a relaxation delay of 20 s, and a linebroadening of 10 Hz were employed. Centerbands are indicated by asterisks (*).

of P_4S_5 and of two polymorphs isolated for the new β - P_4S_6 solid material.

Two P_4S_5 isomers, α - P_4S_5 and β - P_4S_5 , are known.

α - P_4S_5 . During the course of our P_4S_n investigations Harris et al.¹³ reported ^{31}P MAS and solution-state NMR data for α - P_4S_5 . While their ^{31}P MAS data are in good agreement with our results (Table III), the solution-state data are based on the assignment by Thamm et al.³ The apparently large differences between the ^{31}P chemical shifts for the solid and solution state observed by Harris et al.¹³ were somewhat surprising to and could not be accounted for by the authors. However, with the reassignment of the α - P_4S_5 solution-state spectrum (Table II), obtained from the molten-state exchange study, the chemical shift differences for the phases are much less dramatic. Furthermore, the chemical shift differences for the solution-to-molten-state change show the same trend as those for the solution-to-solid-phase change.

β - P_4S_5 . Contrary to α - P_4S_5 , the free β - P_4S_5 molecule exhibits C_{2v} symmetry, and accordingly the solution-state spectrum shows two triplets. Two polymorphs of β - P_4S_5 were isolated in this work as fine (polymorph A) and large (polymorph B) crystals by crystallization from CS_2 solutions. ^{31}P MAS spectra of the two β - P_4S_5 polymorphs at selected spinning speeds are shown in Figure 6. Our ability to apply stable spinning speeds at any speed in the range up to 10 kHz for 7-mm o.d. rotors was very useful in order to identify all resonances, to avoid serious overlap between centerbands and spinning sidebands (ssb's) or between the ssb's themselves. For the spectrum of β - $\text{P}_4\text{S}_5(\text{A})$ in Figure 6a three

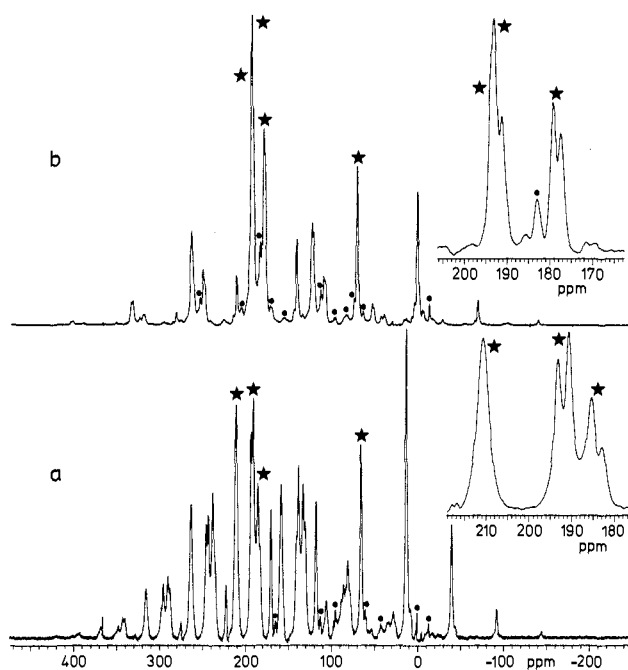


Figure 7. The 121.42 MHz ^{31}P MAS-NMR spectra of two polymorphs of solid β - P_4S_6 : (a) β - $\text{P}_4\text{S}_6(\text{A})$ (200 mg), spinning speed 6365 Hz, 2040 transients and (b) β - $\text{P}_4\text{S}_6(\text{B})$ (200 mg), spinning speed 8500 Hz, 1040 transients. For both spectra 45° pulses of 3- μs pulse width, a relaxation delay of 40 s, and a linebroadening of 10 Hz were employed. Expansions of the 200-ppm region for three of the centerbands, using a slight resolution enhancement, are shown as insets for both spectra. Centerbands are indicated by asterisks (*). In addition to the spinning sidebands, impurity peaks caused by P_4S_7 , β - P_4S_5 , and products of hydrolysis can be seen in both spectra and are indicated by filled circles (●).

singlet resonances are identified at $\delta = 146.4$ (P1,P2), 98.7 (P3 or P4), and 75.4 ppm (P3 or P4) with relative intensities (including ssb's) of approximately 2:1:1, respectively. The assignment immediately follows from the 2D exchange study. These results agree with a published X-ray structure⁴ ($P2_1/m$, $Z = 2$) which shows the asymmetric unit to be one-half of a molecule with the mirror plane through P3-S-P4 and approximate C_{2v} symmetry. However, ^{31}P MAS-NMR clearly establishes that P3 and P4 are inequivalent.

The spectrum of the second polymorph, β - $\text{P}_4\text{S}_5(\text{B})$ (Figure 6b), reveals four resonances of approximately equal intensity: two doublets with equal splitting (expansion in Figure 6b) at $\delta = 152.3$ and 139.8 ppm, respectively, and two singlets at $\delta = 96.5$ and 82.5 ppm, respectively. Assignment of the two doublet splittings to $^1J(\text{P1},\text{P2}) = 230 \pm 10$ Hz (confirmed at 9.4 T) brings the chemical shift assignments for the two polymorphs in mutual agreement (Table III). Thus, in addition to the nonequivalence of P3 and P4 observed for both polymorphs, P1 and P2 are nonequivalent in β - $\text{P}_4\text{S}_5(\text{B})$ because of crystal-packing effects. A similar observation in solid phosphorus sulfides was first made for P_4S_7 ($^1J(\text{P1},\text{P2}) = 232$ Hz).⁵

β - P_4S_6 . Two polymorphs were also isolated for β - P_4S_6 as fine (polymorph A) and large (polymorph B) crystals from CS_2 solutions. Solution-state ^{31}P NMR showed these polymorphs to be

of 90–92% purity with contamination of ca. 2–4% P_4S_7 and ca. 4–8% β - P_4S_5 (see Experimental Section). The ^{31}P MAS spectra of the two β - P_4S_6 polymorphs are depicted in Figure 7. For β - P_4S_6 (A) (e.g., Figure 7a) we identify four resonances of approximately equal intensity and with centerbands at 210.6 (singlet, P4), 191.9 (doublet, P1 or P2), 183.9 (doublet, P1 or P2), and 65.2 ppm (singlet, P3). The assignment follows from the 1D and 2D spectra of the melt containing β - P_4S_6 and from the doublet splittings assigned to $^1J(P1,P2) = 320 \pm 10$ Hz (observed at both 7.1 and 9.4 T). Thus, for β - P_4S_6 (A) P1 and P2 are also inequivalent due to crystal-packing effects. From the different intensities of the centerbands and ssb's for P1 and P2 in Figure 7a it is obvious that their shielding tensor elements differ and are quite sensitive to crystal packing.

For the ^{31}P MAS spectra of β - P_4S_6 (B) (e.g., Figure 7b) a 17-ppm shift toward greater shielding for the P4 singlet relative to its chemical shift in β - P_4S_6 (A) is observed. It thereby coincides with the high-frequency doublet (P1 or P2) observed at 192.0 ppm. The other P1/P2 doublet is observed at 178.6 ppm. Thus, the following four resonances are identified for β - P_4S_6 (B): 193.7 (singlet, P4), 192.0 (doublet, P1 or P2), 178.6 (doublet, P1 or P2), and 70.4 (singlet, P3). Most remarkably the doublet splitting for β - P_4S_6 (B), $^1J(P1,P2) = 225 \pm 15$ Hz, is reduced by about 100 Hz compared to the value observed for β - P_4S_6 (A) but is comparable to $^1J(P1,P2)$ for P_4S_7 and β - P_4S_5 (B). We have presently no explanation for the differences in the magnitudes of $^1J(P1,P2)$ for the two polymorphs of β - P_4S_6 . A single-crystal X-ray study

of β - P_4S_6 (B) (large crystals) shows that the asymmetric unit is one entire molecule ($P1_1/c$, $Z = 4$)¹⁶ consistent with the observation of four resonances in the ^{31}P MAS spectrum.

Concluding Remarks

In conclusion, high-temperature 1D and 2D ^{31}P NMR spectroscopy is shown to be an efficient tool for studying molecular transformations and exchange pathways in melts of β - P_4S_5 or of mixtures of P_4S_3 and sulfur. These studies facilitate chemical shift assignments of earlier incorrectly assigned, unassigned, or unknown solution-state ^{31}P NMR spectra of P_4S_n compounds. Furthermore, the 2D exchange studies in the molten state greatly assist the interpretation of solid-state NMR investigations of P_4S_n compounds. The ability of solid-state ^{31}P MAS-NMR to distinguish and identify new polymorphs and isomers in the series of P_4S_n ($n = 5$ and 6) compounds is demonstrated. Its sensitivity to crystal-packing effects, not obvious from X-ray diffraction, is illustrated to be an important factor in this respect. Such effects lead to observation of ^{31}P - ^{31}P scalar couplings which cannot be determined for the "free" molecules in solution or melt because the P atoms become equivalent due to symmetry.

Acknowledgment. The use of the facilities at the University of Aarhus NMR Laboratory sponsored by the Danish Research Councils SNF and STVF, Carlsbergfondet, and Direktør Ib Henriksens Fond is acknowledged. We thank Aarhus University Research Foundation for equipment grants.

High-Resolution Oxygen-17 NMR of Solid Silicates

K. T. Mueller, Y. Wu, B. F. Chmelka, J. Stebbins,[†] and A. Pines*

Contribution from the Materials and Chemical Sciences Division, Lawrence Berkeley Laboratory, 1 Cyclotron Road, Berkeley, California 94720, and Department of Chemistry, University of California, Berkeley, California 94720. Received June 1, 1990

Abstract: Several ^{17}O -enriched silicates were studied by use of dynamic angle spinning (DAS) and double rotation (DOR) nuclear magnetic resonance spectroscopy. These methods average away second-order quadrupolar interactions by reorienting a sample about a time-dependent axis, thereby yielding high-resolution spectra of oxygen-17 nuclei. A narrow spectral line is observed for each distinct oxygen site at the sum of the isotropic chemical shift and the field-dependent isotropic second-order quadrupolar shift. Resolution is increased by up to 2 orders of magnitude compared to conventional magic angle spinning (MAS) spectra. Crystallographically inequivalent oxygens are now observable as distinct resonances in spectra of polycrystalline silicates such as diopside ($CaMgSi_2^{17}O_6$), wollastonite ($CaSi^{17}O_3$), clinoenstatite ($MgSi^{17}O_3$), larnite ($Ca_2Si^{17}O_4$), and forsterite ($Mg_2Si^{17}O_4$).

Introduction

Solid silicates display an array of structures and phases according to their composition and thermal treatment. As the molar percentage of cations increases, for example, the infinite three-dimensional framework of crystalline silica (SiO_2) gives way to more compact chains of Si-O atoms (pyroxenes and amphiboles) and discrete anionic species (orthosilicates and cyclosilicates). Such variations in microstructure can have significant impact on the macroscopic properties of silicate species.¹ Adsorption and reaction processes of porous aluminosilicates, such as zeolites, are tied closely to their local structure, influencing their use as catalysts, selective adsorbents, and ion-exchange media in a variety of important industrial processes.² Furthermore, the abundance of silicon and oxygen in the Earth's crust³ makes physicochemical

studies of solid silicates important for understanding many natural geochemical processes.

The microstructure of silicates can be probed by examining the electromagnetic environment of their nuclei with the use of nuclear magnetic resonance (NMR) spectroscopy. Nearby electrons influence the local magnetic field at the nucleus by both paramagnetic and diamagnetic mechanisms, so that measurement of the shielding (chemical shift) tensor at a specific site is a sensitive probe of the local bonding.⁴ A nucleus with a nonspherical charge

(1) Deer, W. A.; Howie, R. A.; Zussman, J. *Rock-Forming Minerals*; Halsted Press: New York, 1978; Vols. 1, 2.

(2) Breck, D. W. *Zeolite Molecular Sieves: Structure, Chemistry and Use*; Robert E. Krieger: Malabar, FL, 1984.

(3) Douglas, B.; McDaniel, D. H.; Alexander, J. J. *Concepts and Models of Inorganic Chemistry*, 2nd ed.; Wiley: New York, 1983; pp 237–241.

(4) Kirkpatrick, R. J. In *Spectroscopic Methods in Mineralogy and Geology*; Mineralogical Society of America, Reviews in Mineralogy; Hawthorne, F. C., Ed.; Mineralogical Society of America: Washington, D.C., 1988; Vol. 18, pp 341–403 and references therein.

* To whom correspondence should be addressed at the University of California.

[†] Address: Department of Geology, Stanford University, Stanford, CA 94305.